Available online at www.sciencedirect.com
ScienceDirect
Biochimica et Biophysica Acta 1763 (2006) 1298–1306
BIOCHIMICA ET BIOPHYSICA ACTA
BBA
www.elsevier.com/locate/bbamcr

Biophysical characterization of S100A8 and S100A9 in the absence and presence of bivalent cations

Thomas Vogl [a], Nadja Leukert [a], Katarzyna Barczyk [a], Kerstin Strupat [b], Johannes Roth [a,c,d,*]

[a] Institute of Experimental Dermatology, University of Muenster, Roentgenstr. 21, 48149 Muenster, Germany
[b] Thermo Electron GmbH, Hanna-Kunath-Str. 11, 28199 Bremen, Germany
[c] Department of Pediatrics, University of Muenster, Albert-Schweizer-Str. 33, 48149 Muenster, Germany
[d] Interdisciplinary Center of Clinical Research, University of Muenster, Albert-Schweizer-Str. 33, 48149 Muenster, Germany

Received 17 July 2006; received in revised form 18 August 2006; accepted 18 August 2006
Available online 25 August 2006

Abstract

S100A8 and S100A9 are two proinflammatory molecules belonging to the S100 family of calcium-binding proteins. Common to all S100 proteins S100A8 and S100A9 form non-covalently associated complexes which have been shown to exhibit different functional properties. Besides dimerization, recent research is focused on the importance of higher oligomeric structures of S100 proteins induced by bivalent cations. While S100A8/S100A9-heterodimers are formed in the absence of calcium, tetramerization is strictly calcium-dependent. Heterodimer formation is not a simple process and our biophysical analyses (FRET, ESI-MS) demonstrate that simply mixing both subunits is not sufficient to induce complex formation. Steps of denaturation/renaturation are necessary for the recombinant complex to show identical biophysical properties as S100A8/S100A9 obtained from granulocytes. In addition to calcium both proteins are able to bind zinc with high affinity. Here we demonstrate for the first time by different biophysical methods (MALDI-MS, ESI-MS, fluorescence spectroscopy) that zinc-binding, like calcium, induces $(S100A8/S100A9)_2$-tetramers. Using mass spectrometric investigations we demonstrate that zinc triggers the formation of $(S100A8/S100A9)_2$-tetramers by zinc-specific binding sites rather than by interactions with calcium-specific EF-hands. The zinc-induced tetramer is structurally very similar to the calcium-induced tetramer. Thus, like calcium, zinc acts as a regulatory factor in S100A8/S100A9-dependent signaling pathways.

Keywords: Calcium-binding proteins; MRP8; MRP14; Calgranulin; Calprotectin; Complex formation; Calcium; Zinc

1. Introduction

S100A8 (myeloid related protein 8, MRP8) and S100A9 (MRP14) belong to the multifunctional calcium-, zinc- and copper-binding S100 protein family. Members of this family show a divergent pattern of cell- and tissue-specific expression, of subcellular localizations, of post-translational modifications and of affinities for bivalent cations, consistent with their pleiotropic intra- and extracellular functions [1].

S100A8 and S100A9 are specifically expressed in circulating neutrophils and early differentiation stages of monocytes [2] as well as in keratinocytes and epithelial cells under inflammatory conditions [3,4]. During activation of phagocytes both proteins are released by a novel secretory pathway [5], suggesting both intra- as well as extra-cellular functions during inflammation.

Common to other S100 proteins, S100A8 and S100A9 form dimers as well as higher order oligomers. While S100A8/S100A9-heterodimers are formed in the absence of calcium, tetramerization is strictly calcium-dependent [6] and therefore dependent on a functional C-terminal EF-hand in S100A9 as demonstrated by mutagenesis [7]. Oligomerization of S100 proteins in the presence of bivalent cations becomes more and more the focus of research since polymers of S100B [8] and S100A12 [9] are described in receptor assembly during RAGE-mediated signaling, while calcium-induced $(S100A8/S100A9)_2$-tetramers were shown to play a role in tubulin polymerization and stabilization during activation of phagocytes [7,10]. Nevertheless, a proper dimerization is essential for tetramerization as demonstrated by our investigations (FRET, mass spectrometry).

* Corresponding author. Institute of Experimental Dermatology, University of Muenster, Roentgenstr. 21, D-48149 Muenster, Germany. Tel.: +49 251 83 56578; fax: +49 251 83 57192.
E-mail address: rothj@uni-muenster.de (J. Roth).

0167-4889/$ - see front matter © 2006 Elsevier B.V. All rights reserved.
doi:10.1016/j.bbamcr.2006.08.028

Structurally S100A8 and S100A9 are characterized by two calcium-binding sites of the EF-hand type and the dimer is known to bind four Ca^{2+}-ions. Besides calcium S100A8/S100A9 are also able to bind zinc with high affinity. The zinc-binding motive of S100A8/S100A9 is not yet identified but both proteins contain HEXXH motives in their sequences that are putative zinc-binding sites [11]. The zinc-binding sites of S100B, S100A2 and S100A7 have been already characterized based on mutational analysis, NMR data and crystal structures [12–14]. These S100 proteins bind two Zn^{2+}-ions per homodimer and the zinc-binding sites are formed by residues from both subunits. Since the zinc-binding residues in S100A7 are fully conserved in S100A9 one can suggest that the S100A8/S100A9-dimer coordinates zinc in a similar way as S100A7 [14,15]. It has been shown that extracellular S100A8/S100A9 exhibits antimicrobial activity just by chelation of zinc [11], which is necessary for growth of bacteria. Tested alone, neither S100A8 nor S100A9 showed antimicrobial activity. Only when both proteins were used in combination zinc-reversible activity could be demonstrated, suggesting that the heterodimer of S100A8 and S100A9 is necessary to form a zinc-binding site capable of inhibiting microbial growth. However little is known about oligomeric structures of S100A8/S100A9 induced by zinc. Using biophysical methods (MALDI-MS, ESI-MS and fluorescence spectroscopy) we now show a zinc-induced S100A8/S100A9-tetramerization. We demonstrate that zinc triggers the formation of $(S100A8/S100A9)_2$-tetramers by zinc-specific binding sites rather than by interactions with calcium-specific EF-hands and we further demonstrate that the zinc-induced tetramer is structurally very similar to the calcium-induced tetramer. Thus we propose that besides calcium, zinc acts as a regulatory factor in S100A8/S100A9-dependent signaling pathways.

2. Materials and methods

2.1. Expression and purification of S100A8 and S100A9

S100A8 and S100A9 were isolated from human granulocytes (gr) as a heterodimer and purified according to Vogl et al. [6]. It should be noted, that two main isoforms of S100A9 are known: the full length form of S100A9 and S100A9*. The second one (S100A9*) is shorter by the first four N-terminal amino acids due to alternative translation. Therefore three different combinations of tetramers can be detected for S100A8/S100A9 from granulocytes while for the purified recombinant complex only a single peak is expected. Samples ($[S100A8/S100A9]_{stock}$ = 50 μM) were stored in 10 mM NH_4Ac, 2 mM DTT, pH 7.4 or dialysed against the buffer of choice.

Recombinant human (rh) S100A8 and rhS100A9 were expressed in E. coli BL21 (DE3) separately from each other and subsequently purified as described by Leukert et al. [7]. For the mass spectrometric investigations both proteins were stored separately from each other in 10 mM NH_4Ac, 2 mM DTT, pH 7.4.

Protein concentrations were determined by UV absorption at 280 nm using specific absorption coefficients of 1.03 ml mg^{-1} cm^{-1} (for S100A8), 0.526 ml mg^{-1} cm^{-1} (for S100A9) and 0.75 ml mg^{-1} cm^{-1} (for the complex).

Complex formation of rhS100A8 and rhS100A9 was enabled by two ways: Both proteins were mixed in an equimolar mixture ($[rhS100A8/rhS100A9]_{stock}$ = 50 μM) and incubated for 1 h at room temperature to allow complex formation. In another approach a denaturation/renaturation step was included. Samples were adjusted to pH 2.0–2.5 by adding hydrochloric acid in 0.1 M glycine buffer. After 60 min incubation at room temperature, samples were dialyzed stepwise to get adapted to 20 mM Tris (pH 8.5), 1 mM EDTA, 1 mM EGTA, 2 mM DTT for proper refolding and complex formation. After centrifugation (10 min, 60,000×*g*, 4 °C) to pellet aggregated material, samples were applied to anion exchange column chromatography. Only fractions which contained equal amounts of both proteins, as detected by SDS-PAGE, were collected. Samples were stored as stock solutions at −20 °C. Correct refolding and complex formation was assessed by SDS-PAGE, CD spectroscopy, MALDI-MS and ESI-MS [7].

2.2. Labeling of S100A8 and S100A9 by Cy3 and Cy5

Following the instructions of the labeling kit (FluoroLinkTM Cy3 (PA23000) and Cy5 (PA25000), Amersham Pharmacia) rhS100A8 and rhS100A9 were labelled with amine-reactive Cy3 (donor) or Cy5 (acceptor) separately, and the final dye/protein ratios were estimated. For the Cy3- and Cy5-reactive dyes, the final ratios of dye/protein assembly were rhS100A9–Cy5 = 3.0, rhS100A9–Cy3 = 2.5, rhS100A8–Cy3 = 2.2 and rhS100A8–Cy5 = 3.3, respectively.

2.3. Fluorescence resonance energy transfer (FRET) measurements

Time-based emission, steady-state emission and excitation spectra were collected using a spectrofluorometer (Spex, Model FluoroMax II, Instruments SA, Munich Germany). The donor fluorophore (Cy3) was excited at 550 nm, and the acceptor fluorophore (Cy5) was recorded at the emission wavelength of 670 nm (5 nm band pass). To avoid photobleaching samples were only excited at the time points indicated. Measurements were performed using a 70-μl fluorescence cuvette with 10 mm excitation and 3 mm emission path lengths. For steady-state spectra, Cy3 and Cy5 excitation and emission scans were collected between 400 and 700 nm.

2.4. Fluorescence measurements of S100A8/S100A9

Fluorescence spectra were recorded at 20 °C with a spectrofluorometer (Spex, Model FluoroMax II, Instruments SA, Munich Germany) using protein concentrations of 5 μg/ml (0.208 μM). The excitation wavelength was 280 nm with a bandpass of 1 nm, and the emission scans were recorded as indicated in the figures with a bandpass of 4 nm and an integration time of 0.2 s. To avoid possible disulfide formation between S100A8 and S100A9, 1 mM DTT was added to the buffer (20 mM Tris, pH 7.5 at 20 °C). All fluorescence spectra were buffer corrected. For titration of S100A8/S100A9 with zinc and copper, the fully reduced complex was used in the absence of free reducing agents. Ca^{2+}-, Cu^{2+}- or Zn^{2+}-binding to the complex were monitored by the change in the intrinsic Trp and Tyr fluorescence. Ion concentrations ranging from 0 to 50 μM were used for the titration. All samples were preequilibrated overnight prior to the fluorescence measurements. The changes in the fluorescence maximum were plotted as a function of the Ca^{2+}-, Cu^{2+}- or Zn^{2+}-concentration as indicated.

2.5. Circular dichroism (CD) spectroscopy of S100A8/S100A9

CD spectra of S100A8/S100A9 in the absence and presence (10 and 100 μM) of bivalent cations were recorded from 205 to 260 nm in a 0.1 cm cuvette in a CD spectrophotometer type CD6 (Jobin Yvon, Paris, France). The buffer of the S100A8/S100A9 solution was changed to 20 mM Tris (pH 7.5) by extensive dialysis. Cations were added and samples were incubated for equilibrium over night at 4 °C. All spectra were averaged over five scans and corrected for the buffer signal. For all measurements, buffers were degassed and the sample compartment was thoroughly purged with a constant flow of nitrogen (5 l min^{-1}). Temperature was controlled by a self-constructed Peltier element cuvette holder.

2.6. ESI-MS

Sample analysis was performed under both, denaturing and native solvent conditions. Denaturing solvent conditions were chosen to determine the molecular masses of single protein chains involved. A mixture of bidistilled water/acetonitrile formic acid (49.5/49.5/1, v/v/v) was prepared in which the

samples were diluted to [S100A8/S100A9]=2–5 μM and subsequently mass analyzed by ESI-MS. Native solvent conditions were chosen to determine the oligomerization state of the protein chains in both the presence and absence of Ca^{2+}-and/or Zn^{2+}-ions. For this purpose the stock solutions were diluted to [S100A8/S100A9]=10 μM in 10 mM NH_4Ac, 2 mM DTT, pH 7.4. For experiments in the presence of bivalent ions, Ca^{2+}- or Zn^{2+}-ions were added to a final ratio of 6 Ca^{2+}-ions per calcium-binding site (CaBS) and/or 6 Zn^{2+}-ions per zinc-binding site (ZnBS).

A Micromass Q-TOF instrument equipped with a nano-spray z-spray source using in-house made glass capillaries was used. The interfacial pressure was set to p_{int}=1.5 mbar and the cone voltage was set to V_c=125 V as described earlier in more detail [16].

2.7. MALDI-MS

To mass analyze samples under denaturing conditions the super-DHB matrix was prepared by mixing an aqueous 15 g l^{-1} solution of 2,5-dihydroxybenzoic acid (DHB) with a 15 g l^{-1} ethanol solution of 2-hydroxy-5-methoxy benzoic acid (both Aldrich, Steinheim, Germany), in the ratio of 9/1 (v/v) [6]. The MALDI-matrix 2,6-dihydroxy acetophenon (2,6-DHAP) was used to analyze the complex formation in the absence and presence of bivalent cations. 2,6-DHAP was prepared freshly every day as a saturated solution in a mixture of bidistilled water/acetonitrile (8/2, v/v). The matrix was sonicated for 5 min and undissolved matrix material was centrifuged shortly. Supernatant was used as matrix. As described for the ESI-MS experiment, the sample stock solutions were diluted to [S100A8/S100A9]=10 μM in 10 mM NH_4Ac, 2 mM DTT, pH 7.4 and measured in both the absence and presence of bivalent ions. For experiments in the presence of bivalent ions, Ca^{2+}- or Zn^{2+}-ions were added. Finally, 6 Ca^{2+}-ions per calcium-binding site (CaBS) and/or 6 Zn^{2+}-ions per zinc-binding site (ZnBS) were provided. Typically, 0.5 μl of the analyte solution and 2 μl of the matrix solution were pipetted onto the target and air dried. In order to detect the specific complex formation (2,6-DHAP matrix), only first shot mass spectra onto a given location were accumulated according to previous results [6]. A home-built UV-DE-Reflector-TOF instrument equipped with a post acceleration held on − 20 kV followed by a secondary electron multiplier was used for MALDI-mass spectra acquisition.

2.8. DSC

Data obtained by Differential Scanning Calorimetry (DSC) were used to compare the stabilities of granulocytic S100A8/S100A9 and rhS100A8/rhS100A9 as well as for the subunits in the absence and presence of Ca^{2+}-ions. For each sample a concentration of 42 μM was chosen. The temperature dependence of the apparent molar heat capacity was determined using a differential scanning microcalorimeter (Nano-DSC, Calorimetric Science Corp. (CSC)). Data were collected automatically by a PC. Apparent molar heat capacity (C_p) and temperature were registered in 0.1 K steps; the heating rate employed was 2 K min^{-1}. Each protein run was preceded by a calibration run with buffer filled cells to establish the baseline.

2.9. DLS

Data of Dynamic Light Scattering (DLS) were accumulated with a Dynapro-801 molecular sizing instrument. Data processing was performed by the program Dynamics 5.25 and the DynaLS software (Protein Solutions). The software relates the molecular mass (m) of a protein to its hydrodynamic radius (R_h) measured in solution by the following equation: $m=4/3\ \pi\ N_A\ (R_h/f)^3/\varsigma$ in which N_A is Avogadro's constant [mol^{-1}], f=1.25707 is the frictional factor, R_h is the hydrodynamic radius [μm] and ς=0.726 is the specific protein volume [g/cm^3].

3. Results and discussion

3.1. Complex formation of recombinant S100A8 and S100A9

In a first approach we tested whether simple mixing of both recombinant expressed subunits is sufficient for heterodimer formation by FRET analyses. The fluorescent dyes Cy3 and Cy5 were covalently coupled to rhS100A8 and rhS100A9, respectively. Excitation and emission scans of rhS100A8–Cy3 and rhS100A9–Cy5 are shown in the inset of Fig. 1. For a better presentation all spectra are normalized to the same level. After mixing of fluorescent labelled rhS100A8–Cy3 and rhS100A9–Cy5 we observed only a small increase in fluorescence at 670 nm over time (excitation wavelength: 550 nm), indicating no significant interaction of the subunits. In the presence of 1 mM $CaCl_2$ we observed a faster and stronger increase in fluorescence intensity for up to 1 h where the signal persisted (Fig. 1). These data indicate that complexes are formed in the presence of calcium. However, this process takes a long time and the quality of complex formation remains questionable. For the combination rhS100A8–Cy5–rhS100A9–Cy3 similar results were obtained (data not shown).

In a recent work we have described the oligomerization pattern of native S100A8 and S100A9 derived from human granulocytes by ESI-MS [16]. Using the same conditions for rhS100A8 and rhS100A9 we were neither able to detect heterodimers in the absence of calcium nor heterotetramers in the presence of calcium (Fig. 2A–D). Thus, it is obvious that simple mixing of the recombinant subunits is not sufficient for proper complex formation.

In the next step we included a denaturation/renaturation step in order to enable the recombinant proteins to fold properly during the renaturation step and to compare the oligomerization behaviour with the known data obtained from granulocytic S100A8/S100A9 [6,16]. For denaturation samples were adjusted to pH 2.0–2.5. After 60 min of incubation at room temperature, samples were stepwise dialyzed to neutral pH for proper refolding and complex formation and subsequently applied to anion exchange column chromatography. Only those fractions were collected that contain equal amounts of both proteins. MALDI-MS as well as ESI-MS [7] were used to analyze the complex formation pattern of rhS100A8/rhS100A9 after the denaturation/renaturation step.

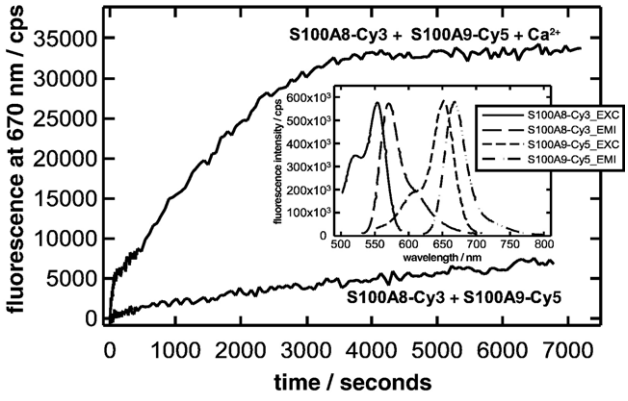

Fig. 1. Detection of dimerization of recombinant S100A8/S100A9 by FRET. Time-based recording of acceptor fluorescence (rhS100A9–Cy5) was carried out immediately after mixing of rhS100A8–Cy3 (0.2 μg/ml) and rhS100A9–Cy5 (0.2 μg/ml) in the absence or presence of up to 1 mM $CaCl_2$. rhS100A8–Cy3 was excited at 550 nm and donor emission was recorded at the emission wavelength of 670 nm (rhS100A9–Cy5). Inset: absorption and emission spectra of rhS100A8–Cy3 and rhS100A9–Cy5.

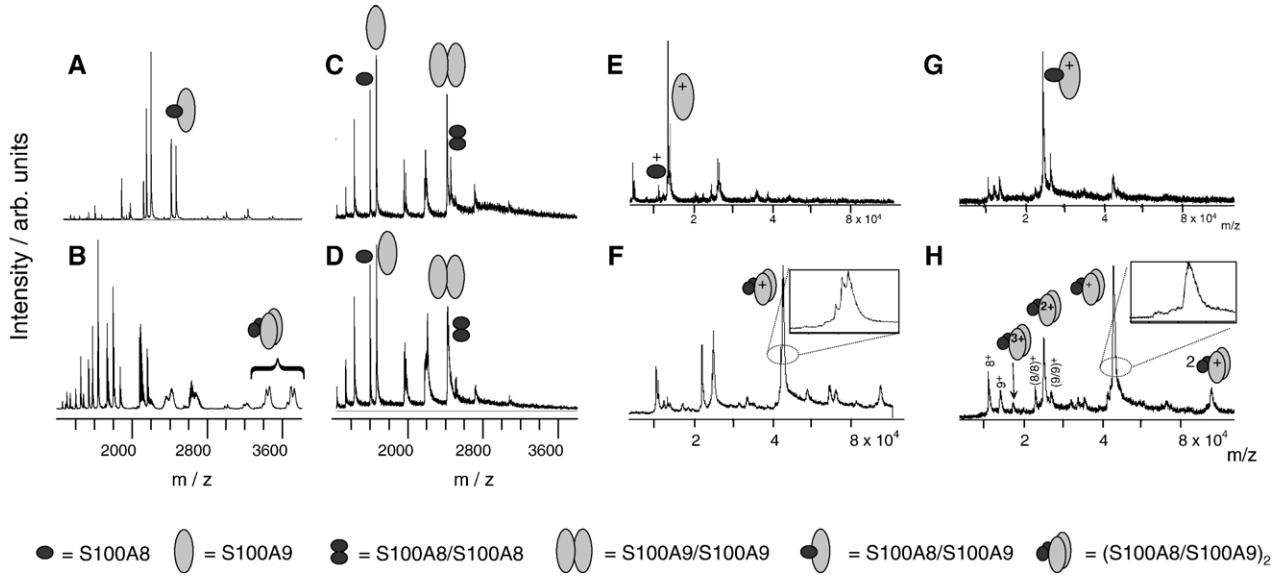

Fig. 2. Nano spray ESI mass spectra and MALDI mass spectra of S100A8/S100A9 in the absence and presence of calcium under native solvent conditions. Panels A and B show ESI mass spectra of S100A8/S100A9 from human granulocytes. The mass spectra between *m/z* 1400 and 3600 are shown. In the absence of calcium (A) the main signals observed correspond to heterodimers. In the presence of calcium (B) signals corresponding to tetramers occurred in the range between *m/z* 3000–3800. Panels C and D show ESI mass spectra of rhS100A8/rhS100A9 without denaturation/renaturation procedure. Neither in the absence (C) nor in the presence (D) of calcium heterodimers or tetramers were found. The main signals correspond to homodimers. Only 1st shot spectra were accumulated and stored for MALDI-MS (E–H). MALDI mass spectra are shown between *m/z* 20,000 and 100,000 together with an inset in f and h between *m/z* 46,000 and 50,000 in the absence (E and G) and presence (F and H) of calcium using 2,6-dihydroxy-acetophenone as matrix. S100A8/S100A9 from human granulocytes show heterodimers in the absence (E) and heterotetramers in the presence of calcium (F). MALDI mass spectra of rhS100A8/S100A9 complexes after denaturation/renaturation procedure as described in Materials and methods show heterodimers in the absence (G) and heterotetramers in the presence (H) of calcium.

Both MS-techniques revealed the expected heterodimerization in the absence and the heterotetramerization in the presence of bivalent ions after the denaturation/renaturation step (Fig. 2E–H, [7]). In Fig. 2E and F results of S100A8/S100A9 from granulocytes in the absence and presence of calcium ions are shown. One can clearly see a peak at 48 kDa representing tetramers of S100A8/S100A9. The inset of Fig. 2F shows the *m/z* range between 46,000 and 50,000 Da and typically the characteristic triple peak of tetramers due to the two isoforms of S100A9, the smaller one (S100A9*) lacking the first four amino acids (TCKM). In first shot spectra of rhS100A8/rhS100A9 derived from denaturation/renaturation steps the base peak represents heterodimers in the absence (Fig. 2G) and heterotetramers in the presence (Fig. 2H) of calcium. It should be noted that the peak at *m/z* 16,000 can only be assigned to the triply charged heterotetramer (T3+), because no other oligomer matches this mass (Fig. 2H). Thus, introduction of a denaturation/renaturation step results in the same oligomerization pattern described earlier for S100A8/S100A9 purified from human granulocytes [6,16]. During refolding of proteins several folding intermediates are formed. One of them, called 'molten globule', is characterized by a fully secondary structure content but without any tertiary contacts. It seems conceivable to improve and facilitate the kinetics of refolding and the yield of renatured protein by the addition of Ca^{2+}-and/or Zn^{2+}-ions. Binding of at least some ions to the specific binding sites would stabilize structural sections and therefore facilitate adequate folding.

Additionally, results from differential scanning microcalorimetry confirmed our assumption of correct complex formation. Fig. 3A shows heat capacity curves for thermal unfolding of S100A8/S100A9 from granulocytes and rhS100A8/rhS100A9 in the absence and presence of calcium (2 mM). All transitions are irreversible (data not shown). However, a simple comparison of the curves is permissible because identical conditions such as heating rate and sample preparation were applied. In the absence of calcium both curves indicate a single transition with a transition temperature $t_{½}$ of 68.7 °C consistent with the presence of only S100A8/S100A9 heterodimers in both samples since presence of additional forms like monomers or homodimers would result in different, independent transitions with different transition temperatures (Fig. 3B). Addition of calcium strongly stabilizes both S100A8/S100A9 preparations resulting in a comparable increase in the transition temperature of +13 °C for granulocytic S100A8/S100A9 and +11 °C for the recombinant complex. This shift indicates induction of strong non-covalent interactions in the S100A8/S100A9 complex. The small differences in the transition temperatures in the presence of calcium between the different S100A8/S100A9 preparations are not significant and do not indicate relevant differences between granulocytic and recombinant preparations of S100A8/S100A9.

Surprisingly, the unfolding transitions of the individual subunits were completely different despite of close structural homology. For rhS100A8 an unfolding transition was observed with high cooperativity and $t_{½}$ of 59.9 °C in the absence and of $t_{½}$ of 65.8 °C in the presence of 2 mM calcium. The transition temperature $t_{½}$ of 52.8 °C of rhS100A9 was much lower and due to the broadness of the denaturation curve the cooperativity of the transition is much lower than observed for rhS100A8 or the heterodimeric complex. The presence of

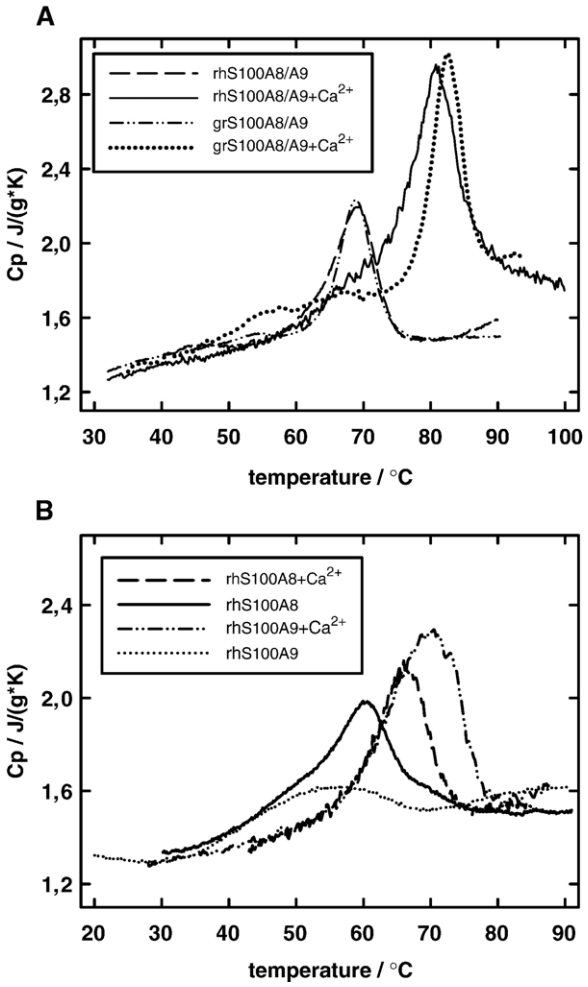

Fig. 3. Experimental heat capacity curves of unfolding of grS100A8/S100A9, rhS100A8/rhS100A9 (A) and individual subunits (B) in the absence and presence of 2 mM Ca^{2+}-ions. Heating rate: 2 °C min^{-1}. Protein concentration: 42 μM. Each measurement was reproduced at least twice.

2 mM calcium leads to a significant thermal stabilization of rhS100A9, which results in an increase in the transition temperature of +17.2 °C (from 52.8 to 70.0 °C) and a higher cooperativity.

The molecular mechanisms of the strong induction of thermal stabilization of rhS100A9 in the presence of calcium are currently not clear. Recently, the 3D-structure of rhS100A9 was analysed by NMR studies and by X-ray crystallography [17,18]. In both studies the C-terminus could not be resolved most probably due to its high flexibility. This long C-terminus is unique for S100A9 and is not found in other S100 proteins. The flexibility of the S100A9 C-terminus may destabilize the protein as indicated by the heat capacity curve for S100A9 in the absence of calcium (Fig. 3B). In the presence of calcium both S100A8 and S100A9 are stabilized as indicated by higher transition temperatures for both subunits. However, it may be speculated that the stronger thermal stabilization of rhS100A9 in the presence of calcium may arise from a restriction of the flexibility of the C-terminus.

Earlier data obtained by X-ray studies indicated, that both S100A8 as well as S100A9 are able to form homodimers in the absence of their binding partner [18,19], while in the presence of both subunits formation of the heterodimer is highly preferred [17,20]. However, the high thermal stability of both individual subunits in vitro (Fig. 3B) may interfere with proper heterodimer formation after simple mixing of rhS100A8 and rhS100A9. These data indicate that characterization of proper complex formation by biophysical methods and/or functional assays is a prerequisite for studies using rhS100A8 and rhS100A9 in biological assays [7,10]. Some of the controversial results regarding biological functions of S100A8 and S100A9 as chemotaxis or other effects on target cells published during the last years may be explained by undefined contaminations of monomers and/or homodimers in the preparations used by different groups [17,21–26].

3.2. Oligomeric pattern of S100A8/S100A9 in the presence of calcium

There is still a conflict in the literature concerning the oligomerization state of both proteins. Meanwhile it is commonly accepted that human S100A8 and S100A9 form stable heterodimers in the absence of calcium, while oligomerization states of both proteins in the presence of calcium are discussed controversially; heterodimers, homodimers and trimers have been described earlier. By mass spectrometric studies we have shown that the oligomerization state of both proteins in the presence of calcium is solely a $(S100A8/S100A9)_2$-heterotetramer (see also Fig. 2) [6,7,16]. Nevertheless we investigated the oligomerization states of S100A8/S100A9 in dependence of calcium by dynamic light scattering (DLS) studies. This method has the advantage that artefacts caused by matrix effects, special buffer conditions or other factors affecting the protein samples are excluded. A volume shape hydration model (molecular range between 24 and 110 kDa) was chosen according to the known structures of S100 proteins so far. Fig. 4 shows the DLS results of

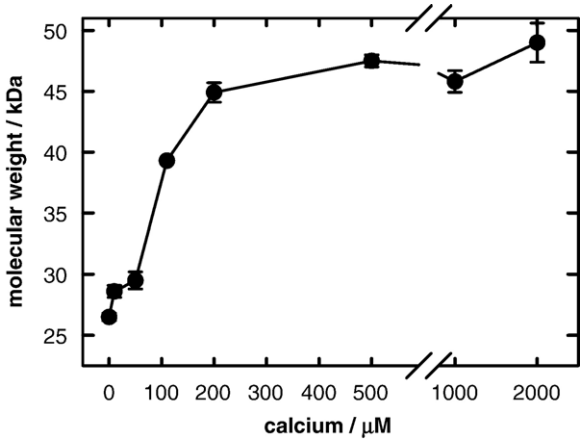

Fig. 4. Analysis of the oligomeric structure of S100A8/S100A9 at increasing Ca^{2+}-concentrations by DLS. The hydrodynamic radius R_h of S100A8/S100A9 was monitored as a function of Ca^{2+} by DLS. A volume shape hydration model (model average 24–110 kDa) was used to calculate the molecular weight of S100A8/S100A9 from the hydrodynamic radius R_h as described in Materials and methods.

S100A8/S100A9 at increasing calcium concentrations confirming the occurrence of the heterodimer in the absence and formation of a tetramer in the presence of calcium. In the absence of calcium a molecular mass of 26.5±0.5 kDa for S100A8/S100A9 was calculated from the hydrodynamic radius. This value agrees well with the theoretical mass for the S100A8/S100A9-heterodimer of 24 kDa indicating that the chosen model is valid. In the presence of calcium the hydrodynamic radius for S100A8/S100A9 increases up to 3.01±0.02 nm (47.5±0.3 kDa) describing the tetramer exactly. Recently the calcium induced tetramer of S100A8/S100A9 was also resolved by X-ray crystallography (PDB file: 1XK4, Online access: http://www.rcsb.org/pdb/Welcome.do). As soon as structural details are available for the reasons of heterotetramer formation our assumption on restricting the flexible S100A9 C-terminus by binding of calcium should be answered. Nevertheless, heterodimerization and tetramerization has been confirmed by independent methods and fits well with the structural data obtained earlier by NMR-analyses and yeast two-hybrid analyses [17,20].

3.3. Zinc-induced oligomerization of S100A8/S100A9

In addition to calcium, several S100 proteins are able to bind Zn^{2+}- or Cu^{2+}-ions with different affinities [1]. Distinct calcium- and zinc-binding sites have been described and in

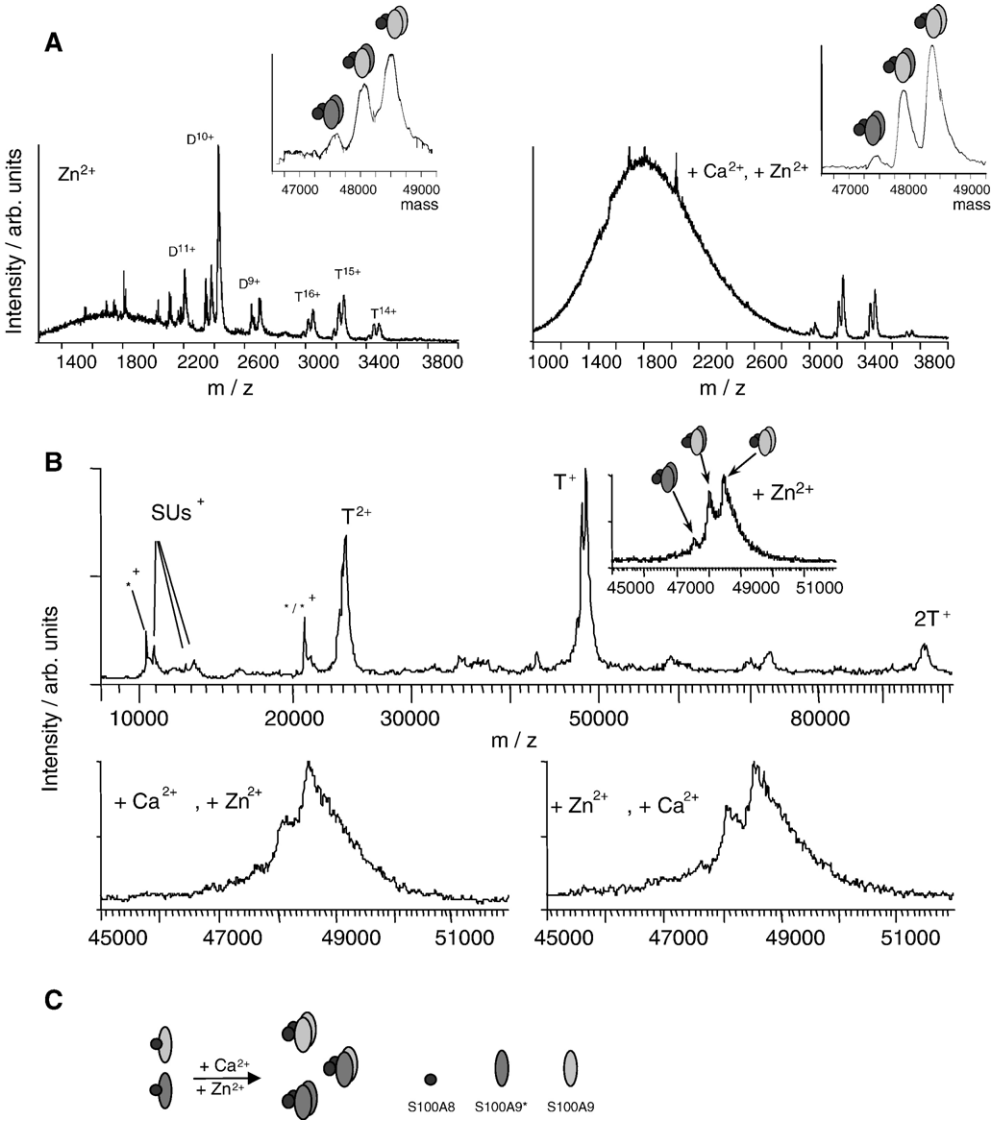

Fig. 5. Analysis of the oligomeric structure of S100A8/S100A9 in the presence of Zn^{2+}-ions and Zn^{2+}/Ca^{2+}-ions. (A) Nano-ESI-mass spectra in the presence of Zn^{2+}-ions (left), and in the presence of Ca^{2+}- and Zn^{2+}-ions (right), both as raw data and transformed spectra (inset). Especially in the presence of both cations S100A8/S100A9 tends to aggregate as can be seen by the hump visible in both raw data spectra between *m/z* 1200 and 2400. (B) UV-MALDI-mass spectra in the presence of Zn^{2+}-ions (top), first Ca^{2+}- and then Zn^{2+}-ions (bottom left), and vice versa (bottom right), using 2,6-dihydroxy-acetophenone as matrix. Inset: resolved MALDI mass spectra between *m/z* 46,000 and 50,000. *S100A12, known contamination in S100A8/S100A9 preparation from granulocytes [33]. Subunits (SUs): S100A8, S100A8ox, S100A9*, S100A9 Tetramers (T): $(S100A8/A9^*)_2$, (S100A8/A9*S100A8/A9), $(S100A8/A9)_2$ (C) Schema of S100A8/S100A9-tetramerization in the presence of bivalent cations proposed from former studies [6,16] and the present investigation.

some S100 proteins the presence of Zn^{2+}-ions modifies the affinity for Ca^{2+}-ions. For S100B [27], S100A2 [28], S100A3 [29], S100A6 (calcyclin) [30], S100A7 [14], S100A8/S100A9 [11,31] and S100A12 (calgranulin C) [32] zinc-binding was reported.

For S100A7 the observed zinc-binding sites are located at the dimer interface and are formed by residues from both subunits. Recently a zinc-induced tetramer consisting of two S100A2 homodimers has been described [13], however nothing is known about the influence of zinc on oligomerization of S100A8 and S100A9. We therefore investigated the zinc-dependent oligomeric pattern of S100A8 and S100A9 by mass-spectrometric analyses.

Our mass spectrometric investigations show that tetramer formation of S100A8/S100A9 is also induced in the presence of zinc. The tetramer is composed of two heterodimers as described earlier for the calcium-induced tetramer (Fig. 5 and Table 1). Eight Zn^{2+}-ions per tetramer can be detected in the absence of calcium using MALDI-MS and twelve Zn^{2+}-ions employing ESI-MS. Compared to the MALDI-MS data ESI-MS might be more sensitive to detect non-covalent interactions of S100A8/S100A9 and Zn^{2+}-ions. Zn^{2+}-ions might bind not exclusively to specific zinc-binding sites but may interact also with four (MALDI) or all (ESI) of the eight calcium-binding sites (EF-hands). This assumption is confirmed by the fact that Ca^{2+}-ions are able to replace Zn^{2+}-ions in all 8 EF-hands (Table 1). It is well known that non-covalent complexes are easier detected and confirmed by ESI-MS than by MALDI-MS. Although we used native and neutral conditions for both methods the crystallization matrix necessary for MALDI-MS may be the reason for a detachment of loosely bound ions.

No changes in S100A8/S100A9 mass spectra (data not shown) and fluorescence measurements (Fig. 6A) were observed by addition of copper indicating that binding of zinc is specific and is not a general finding for bivalent cations.

The parallel addition of calcium and zinc leads to the formation of $(S100A8/S100A9)_2$-tetramers that bind 8 Ca^{2+}-ions and 4 Zn^{2+}-ions (Fig. 5 and Table 1). Replacement experiments with Zn^{2+}-ions and Ca^{2+}-ions revealed that there are at least 4 specific zinc-binding sites per tetramer which are distinct from the EF-hands (Fig. 5B). As described recently for the calcium-induced $(S100A8/S100A9)_2$-tetramer, binding of calcium to the heterodimer seems to be a cooperative phenomenon leading to strong binding of calcium also to the low affinity calcium-binding sites in S100A8 and S100A9 [6]. We assume a similar mechanism for the zinc/calcium-induced tetramer. If the tetramer is formed by either Zn^{2+}- or Ca^{2+}-ions the specific binding sites should be preformed to facilitate binding of the other ions. However, this question is currently under investigation. As reported earlier for other S100 proteins two zinc-binding sites are formed per dimer [1,13,14,30]. The exact structure of a zinc-binding motive in S100 proteins was characterized first for S100A7 by X-ray crystallography. The crystal structure of zinc-loaded S100A7 shows two zinc-binding sites per dimer different from the calcium-binding sites. The zinc-binding motives are formed by two coordinating histidines (H86, H90) from the C-terminus of one monomer and another histidine (H17) and an aspartate (E24) located in the N-terminus of the other monomer. Sequence comparison suggests that this zinc-binding site is present in a number of S100 proteins including S100A9 and S100A12 and possibly S100B and S100A8 [14]. So it seems to be likely that S100A8/S100A9 coordinates zinc in a similar way as S100A7 which would result in a total of four zinc binding sites per tetramer which is in accordance to our data.

In addition, fluorescence emission data and circular dichroism data of S100A8/S100A9 in the presence of either

Table 1
Oligomerization pattern of S100A8/S100A9

Nano-ESI-MS	$(S100A8/A9^*)_2$	(S100A8/A9*) (S100A8/A9)	$(S100A8/A9)_2$	Remark
no Ca^{2+}, Zn^{2+}	47064	47527	47990	Theoretical mass[a]
$+Zn^{2+}$[b]	47770±50	48255±50	48770±48	11–12 Zn^{2+}-ions bound to the tetramers
Δm	706	728	780	
nr. of Zn^{2+} bound	11.1±0.8	11.5±0.8	12.3±0.8	
$+Ca^{2+}$, $+Zn^{2+}$[b]	47689±25	48152±19	48619±13	4 Zn^{2+}-ions and 8 Ca^{2+}-ions are
Δm	625	625	629	bound to the tetrameric forms
$626 \approx 8\ Ca^{2+}$ plus $4\ Zn^{2+}$ plus one acetate or ammonium acetate				

MALDI-MS	$(S100A8/A9^*)_2$	(S100A8/A9*) (S100A8/A9)	$(S100A8/A9)_2$	Remark
no Ca^{2+}, Zn^{2+}	47064	47527	47990	Theoretical mass[a]
$+Zn^{2+}$[b]	47576±32	48040±28	48498±21	8 Zn^{2+}-ions bound to the tetramers
Δm	512	513	508	
nr. of Zn^{2+} bound,	8.1±0.5	8.1±0.4	8.0±0.3	
$+Ca^{2+}$, time $+Zn^{2+}$, time[b]	47612±24	48087±18	48544±10	4 Zn^{2+}-ions and 8 Ca^{2+}-ions are bound
Δm	548	560	556	to the tetrameric forms.
$+Zn^{2+}$, time $+Ca^{2+}$, time[b]	47626±15	48085±6	48540±14	
Δm	562	558	550	
$555 \approx 8\ Ca^{2+}$ plus $4\ Zn^{2+}$, (557.6)				

[a] Including partial oxidation in S1008.
[b] Average over 5 experiments.

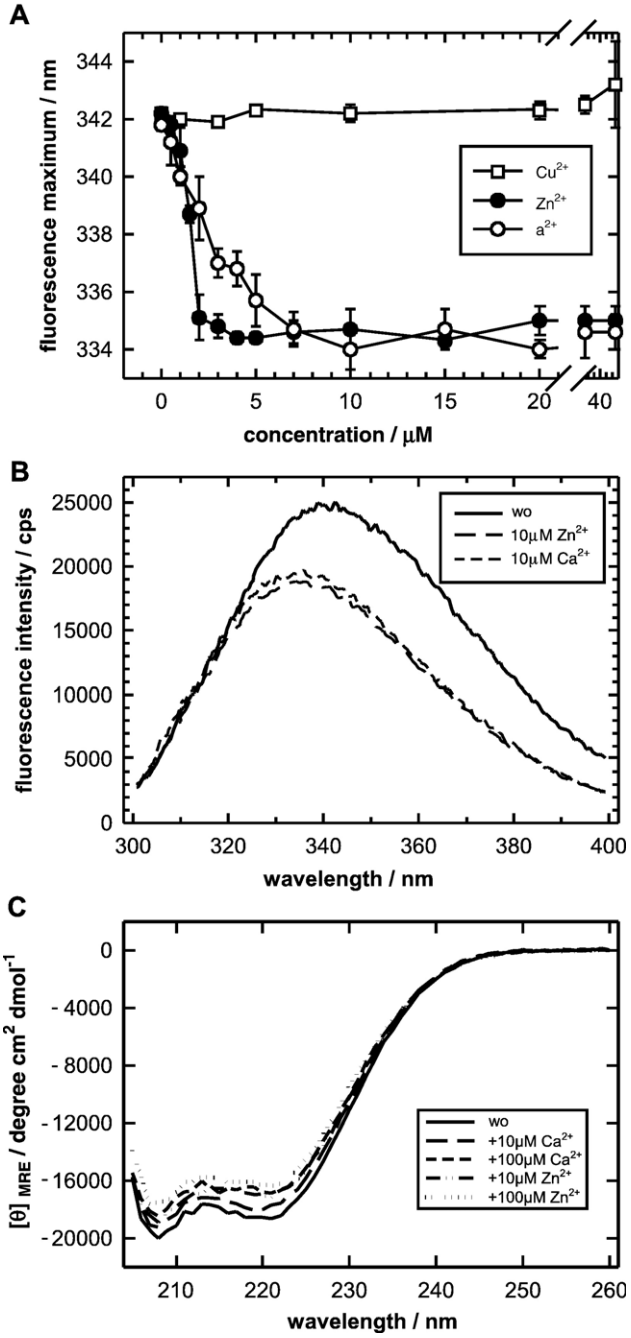

Fig. 6. Structural characterization of S100A8/S100A9 in the absence and presence of bivalent cations. (A) Effects of increasing concentrations of calcium, zinc and copper on Trp and Tyr fluorescence maximum of S100A8/S100A9. Spectra were taken at 20 °C in 20 mM Tris, pH 7.5, 1 mM DTT at a protein concentration of 0.208 µM. All spectra were buffer corrected. After addition of bivalent cations samples were allowed to equilibrate over night at 4 °C (A–C). (B) Fluorescence emission spectra of S100A8/S100A9 in the absence and presence of 10 µM Ca^{2+} or Zn^{2+}, respectively. (C) CD spectra of S100A8/S100A9 complexes in the absence and presence of 10 or 100 µM Ca^{2+} or Zn^{2+}, respectively. The mean residue weight per amino acid of 116.45 was used for calculation of the mean residue ellipticity $[\Theta]_{MRE}$.

Zn^{2+}- or Ca^{2+}-ions indicate that the conformational changes induced by binding of these ions seem to be very similar for both zinc- and calcium-induced tetramers (Fig. 6). As shown in Fig. 6A S100A8/S100A9 complexes significantly undergo a blue shift in intrinsic fluorescence from 342 nm to 334 nm in the presence of increasing calcium and zinc concentrations, while copper showed no effect at all. Tetramer formation in the presence of zinc seems to be more pronounced at lower Zn^{2+}-ion concentrations compared to calcium, however, no significant differences were seen at the "endpoint" of the conformational changes (Fig. 6A). Fig. 6B shows fluorescence emission maxima of S100A8/S100A9 in the presence of Zn^{2+}- or Ca^{2+}-ions in comparison to complexes without bivalent cations. The identical changes in fluorescence intensities of S100A8/S100A9 induced by both cations indicate that zinc and calcium induce similar conformational changes in S100A8/S100A9 complexes resulting in almost identical three-dimensional structures. Furthermore CD-spectra in the absence and presence of bivalent cations exclude major changes in the secondary structure (Fig. 6C) underlining our general assumption that these two cations induce a simple association of two S100A8/S100A9-heterodimers to a $(S100A8/S100A9)_2$-tetramer. Both zinc and calcium are known to be important modulators of inflammatory reactions. Modulation of the pro-inflammatory molecules S100A8 and S100A9 may be a novel molecular mechanism how these proteins regulate inflammatory processes.

4. Conclusion

S100A8 and S100A9 are two S100 proteins which exhibit pro-inflammatory activities in many human diseases. Formation of non-covalently associated complexes is a prerequisite for biological functions and individual complex forms may exhibit different actions. In this regard association of a S100A8/S100A9-heterodimer to a $(S100A8/S100A9)_2$-tetramer is a critical step which is regulated by calcium and zinc in a coordinated matter. Therefore, future studies on biological activities of S100A8 and S100A9 in vivo and in vitro have to consider this point of complex formation carefully.

Acknowledgements

This study has been supported by grants of the Interdisciplinary Center of Clinical Research at the University of Muenster (IZKF Ro2/012/06) and the German Research Foundation (SFB293A16).

References

[1] C.W. Heizmann, J.A. Cox, New perspectives on S100 proteins: a multi-functional Ca(2+)-, Zn(2+)- and Cu(2+)-binding protein family, BioMetals 11 (1998) 383–397.
[2] J. Roth, T. Vogl, C. Sorg, C. Sunderkotter, Phagocyte-specific S100 proteins: a novel group of proinflammatory molecules, Trends Immunol. 24 (2003) 155–158.
[3] N. Hogg, C. Allen, J. Edgeworth, Monoclonal antibody 5.5 reacts with p8,14, a myeloid molecule associated with some vascular endothelium, Eur. J. Immunol. 19 (1989) 1053–1061.
[4] S.E. Kelly, D.B. Jones, S. Fleming, Calgranulin expression in inflammatory dermatoses, J. Pathol. 159 (1989) 17–21.

[5] A. Rammes, J. Roth, M. Goebeler, M. Klempt, M. Hartmann, C. Sorg, Myeloid-related protein (MRP) 8 and MRP14, calcium-binding proteins of the S100 family, are secreted by activated monocytes via a novel, tubulin-dependent pathway, J. Biol. Chem. 272 (1997) 9496–9502.
[6] T. Vogl, J. Roth, C. Sorg, F. Hillenkamp, K. Strupat, Calcium-induced noncovalently linked tetramers of MRP8 and MRP14 detected by ultraviolet matrix-assisted laser desorption/ionization mass spectrometry, J. Am. Soc. Mass Spectrom. 10 (1999) 1124–1130.
[7] N. Leukert, T. Vogl, K. Strupat, R. Reichelt, C. Sorg, J. Roth, Calcium-dependent tetramer formation of S100A8 and S100A9 is essential for biological activity, J. Mol. Biol. 359 (2006) 961–972.
[8] T. Ostendorp, P.M.H. Kroneck, C.W. Heizmann, and G. Fritz, The crystal structure of human S100B reveals a novel octameric assembly; implications for RAGE signalling, 8th Meeting of the European Calcium Society (2004) 122, available online at http://www.ulb.ac.be/assoc/ecs/docs/poster_2_50.doc.
[9] O.V. Moroz, A.A. Antson, E.J. Dodson, H.J. Burrell, S.J. Grist, R.M. Lloyd, N.J. Maitland, G.G. Dodson, K.S. Wilson, E. Lukanidin, I.B. Bronstein, The structure of S100A12 in a hexameric form and its proposed role in receptor signalling, Acta Crystallogr., D Biol. Crystallogr. 58 (2002) 407–413.
[10] T. Vogl, S. Ludwig, M. Goebeler, A. Strey, I.S. Thorey, R. Reichelt, D. Foell, V. Gerke, M.P. Manitz, W. Nacken, S. Werner, C. Sorg, J. Roth, MRP8 and MRP14 control microtubule reorganization during transendothelial migration of phagocytes, Blood 104 (2004) 4260–4268.
[11] P.G. Sohnle, M.J. Hunter, B. Hahn, W.J. Chazin, Zinc-reversible antimicrobial activity of recombinant calprotectin (migration inhibitory factor-related proteins 8 and 14), J. Infect. Dis. 182 (2000) 1272–1275.
[12] P.T. Wilder, K.M. Varney, M.B. Weiss, R.K. Gitti, D.J. Weber, Solution structure of zinc- and calcium-bound rat S100B as determined by nuclear magnetic resonance spectroscopy, Biochemistry 44 (2005) 5690–5702.
[13] M. Koch, T. Ostendorp, M. Gimona, P.M.H. Kroneck, C.W. Heizmann, and G. Fritz, Insights into Zn^{2+}-binding sites in S100 proteins from the crystal structure of Ca^{2+}/Zn^{2+} S100B and spectroscopic investigations of Zn^{2+}-S100A2, 8th Meeting of the European Calcium Society (2004) 101, available online at http://www.ulb.ac.be/assoc/acs/docs/poster_2_28.doc.
[14] D.E. Brodersen, J. Nyborg, M. Kjeldgaard, Zinc-binding site of an S100 protein revealed. Two crystal structures of Ca2+-bound human psoriasin (S100A7) in the Zn2+-loaded and Zn2+-free states, Biochemistry 38 (1999) 1695–1704.
[15] G. Fritz, C.W. Heizmann, 3D structures of the calcium and zinc binding S100 proteins, Handb. Metalloproteins 3 (2004) 529–540.
[16] K. Strupat, H. Rogniaux, D.A. Van, J. Roth, T. Vogl, Calcium-induced noncovalently linked tetramers of MRP8 and MRP14 are confirmed by electrospray ionization-mass analysis, J. Am. Soc. Mass Spectrom. 11 (2000) 780–788.
[17] M.J. Hunter, W.J. Chazin, High level expression and dimer characterization of the S100 EF-hand proteins, migration inhibitory factor-related proteins 8 and 14, J. Biol. Chem. 273 (1998) 12427–12435.
[18] H. Itou, M. Yao, I. Fujita, N. Watanabe, M. Suzuki, J. Nishihira, I. Tanaka, The crystal structure of human MRP14 (S100A9), a Ca(2+)-dependent regulator protein in inflammatory process, J. Mol. Biol. 316 (2002) 265–276.
[19] K. Ishikawa, A. Nakagawa, I. Tanaka, M. Suzuki, J. Nishihira, The structure of human MRP8, a member of the S100 calcium-binding protein family, by MAD phasing at 1.9 A resolution, Acta Crystallogr., D Biol. Crystallogr. 56 (2000) 559–566.
[20] C. Propper, X. Huang, J. Roth, C. Sorg, W. Nacken, Analysis of the MRP8-MRP14 protein–protein interaction by the two-hybrid system suggests a prominent role of the C-terminal domain of S100 proteins in dimer formation, J. Biol. Chem. 274 (1999) 183–188.
[21] P. Ehlermann, K. Eggers, A. Bierhaus, P. Most, D. Weichenhan, J. Greten, P.P. Nawroth, H.A. Katus, A. Remppis, Increased proinflammatory endothelial response to S100A8/A9 after preactivation through advanced glycation end products, Cardiovasc. Diabetol. 5 (2006) 6.
[22] A. Hermani, S.B. De, S. Medunjanin, P.A. Tessier, D. Mayer, S100A8 and S100A9 activate MAP kinase and NF-kappaB signaling pathways and trigger translocation of RAGE in human prostate cancer cells, Exp. Cell Res. 312 (2006) 184–197.
[23] R.A. Newton, N. Hogg, The human S100 protein MRP-14 is a novel activator of the beta 2 integrin Mac-1 on neutrophils, J. Immunol. 160 (1998) 1427–1435.
[24] C. Ryckman, K. Vandal, P. Rouleau, M. Talbot, P.A. Tessier, Proinflammatory activities of S100: proteins S100A8, S100A9, and S100A8/A9 induce neutrophil chemotaxis and adhesion, J. Immunol. 170 (2003) 3233–3242.
[25] K. Sunahori, M. Yamamura, J. Yamana, K. Takasugi, M. Kawashima, H. Yamamoto, W.J. Chazin, Y. Nakatani, S. Yui, H. Makino, The S100A8/A9 heterodimer amplifies proinflammatory cytokine production by macrophages via activation of nuclear factor kappa B and p38 mitogen-activated protein kinase in rheumatoid arthritis, Arthritis Res. Ther. 8 (2006) R69.
[26] K. Vandal, P. Rouleau, A. Boivin, C. Ryckman, M. Talbot, P.A. Tessier, Blockade of S100A8 and S100A9 suppresses neutrophil migration in response to lipopolysaccharide, J. Immunol. 171 (2003) 2602–2609.
[27] J. Baudier, N. Glasser, D. Gerard, Ions binding to S100 proteins. I. Calcium- and zinc-binding properties of bovine brain S100 alpha alpha, S100a (alpha beta), and S100b (beta beta) protein: Zn2+ regulates Ca2+ binding on S100b protein, J. Biol. Chem. 261 (1986) 8192–8203.
[28] C. Franz, I. Durussel, J.A. Cox, B.W. Schafer, C.W. Heizmann, Binding of Ca2+ and Zn2+ to human nuclear S100A2 and mutant proteins, J. Biol. Chem. 273 (1998) 18826–18834.
[29] U.G. Fohr, C.W. Heizmann, D. Engelkamp, B.W. Schafer, J.A. Cox, Purification and cation binding properties of the recombinant human S100 calcium-binding protein A3, an EF-hand motif protein with high affinity for zinc, J. Biol. Chem. 270 (1995) 21056–21061.
[30] J. Kordowska, W.F. Stafford, C.L. Wang, Ca2+ and Zn2+ bind to different sites and induce different conformational changes in human calcyclin, Eur. J. Biochem. 253 (1998) 57–66.
[31] M.J. Raftery, C.A. Harrison, P. Alewood, A. Jones, C.L. Geczy, Isolation of the murine S100 protein MRP14 (14 kDa migration-inhibitory-factor-related protein) from activated spleen cells: characterization of post-translational modifications and zinc binding, Biochem. J. 316 (Pt 1) (1996) 285–293.
[32] E.C. Dell'Angelica, C.H. Schleicher, J.A. Santome, Primary structure and binding properties of calgranulin C, a novel S100-like calcium-binding protein from pig granulocytes, J. Biol. Chem. 269 (1994) 28929–28936.
[33] T. Vogl, C. Propper, M. Hartmann, A. Strey, K. Strupat, C. van den Bos, C. Sorg, J. Roth, S100A12 is expressed exclusively by granulocytes and acts independently from MRP8 and MRP14, J. Biol. Chem. 274 (1999) 25291–25296.